Supplementary materials

To further investigate whether the law between the deflection angle α and the flow field properties is affected by the deflection mode. When the air conditioner is installed in a different pattern, the deflection pattern of the ventilation will also be different. Several common locations for air conditioning arrangements are: the front end of the train, the back end of the train, and the two ends of the train. Its corresponding ventilation deflection modes are: deflection toward the rear end of the cabin (mode 1), deflection toward the front end of the cabin (mode 2), and deflection toward the middle of the cabin (mode 3), as shown in Figure S1.

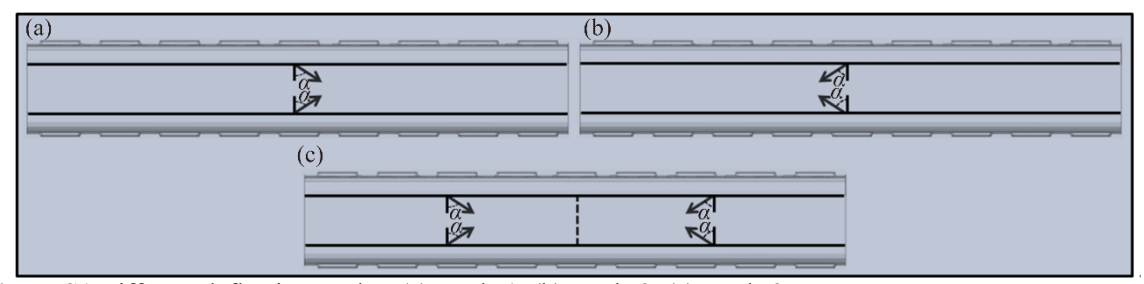


Figure S1 Different deflection modes: (a) Mode 1; (b) Mode 2; (c) Mode 3

1 Typical air distribution

Taking the deflection angles α =15° and α =45° as examples, Figure S2 illustrates the distribution of airflow streamlines in the longitudinal plane for different deflection modes. In mode 1, the streamlines on the cross-section Plane_zm spread out in the positive x-direction. In mode 2, the streamlines on the cross-section Plane_zm spread out in the negative x-direction. In mode 3, the streamlines on cross-section Plane_zm then spread out toward the middle of the cabin. It is worth noting that the streamline diffusion pattern on Plane_zA is the opposite of Plane_zm.

Taking the deflection angles α =15° and α =45° as examples, Figure S3 illustrates the distribution of respiratory pollutants for passengers in different deflection modes. In mode 1, pollutants tend to spread toward the front of the cabin. In mode 2, pollutants tend to diffuse toward the back end of the cabin. In mode 3, pollutants tend to spread to each end of the cabin, bounded by the middle of the cabin. And as the deflection angle α increases, the diffusion inclination of pollutants increases accordingly. These regularities correspond to the streamline distribution in Figure S2.

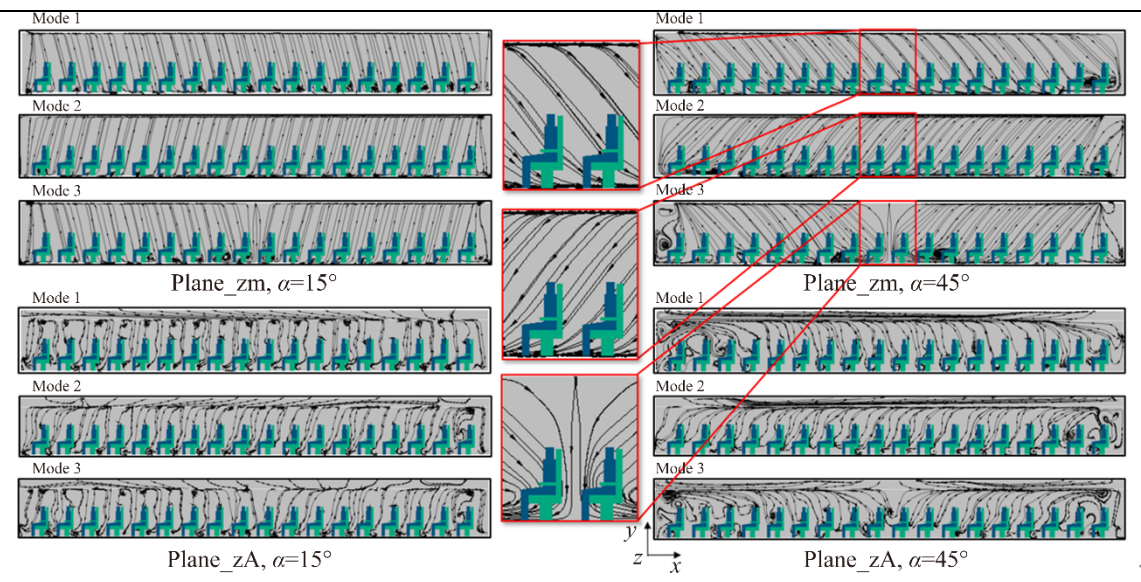


Figure S2 Airflow profile in the longitudinal plane for different deflection modes

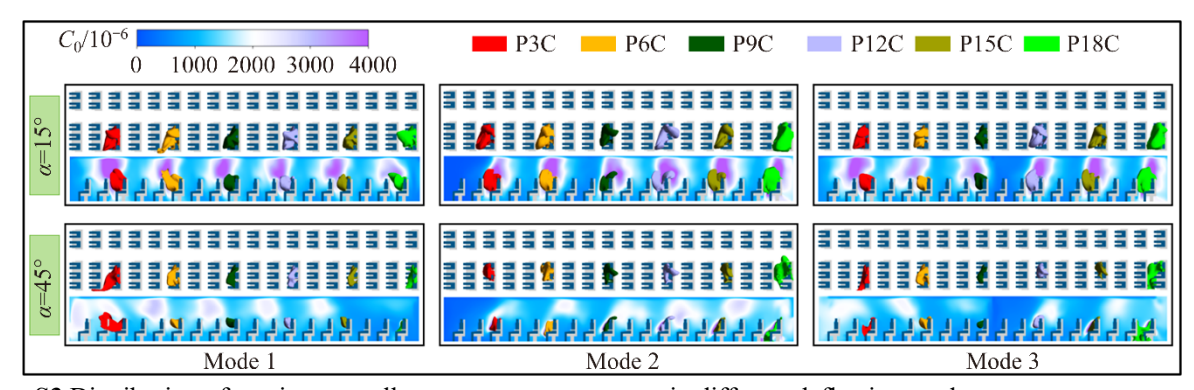


Figure S3 Distribution of respiratory pollutants among passengers in different deflection modes

Taking the deflection angles α =15° and α =45° as an example, Figure S4 illustrates the overall distribution pattern of velocity, temperature, and pollutant concentration in the train cabin for different deflection mode. In mode 1, velocities are relatively high at the back end of the cabin, and temperatures are higher as well as pollutant concentrations at the front end of the cabin. In mode 2, the regularity is completely opposite. In mode 3, velocities are relatively high in the middle of the cabin, and temperatures and pollutant concentrations are higher at the ends of the cabin. Furthermore, this trend is more pronounced as the deflection angle α increases.

2 Evaluation indicators

Figure S5 illustrates the average temperature distribution in the train cabin for different deflection modes and deflection angles. The results show that the temperature in the cabin decreases with the increase of the deflection angle, which is basically consistent with the law shown above. However, the patterns of temperature change among the three models did not show significant differences. Except for the deflection angle α =60°, the average temperature in the cabin was essentially the same for all three modes.

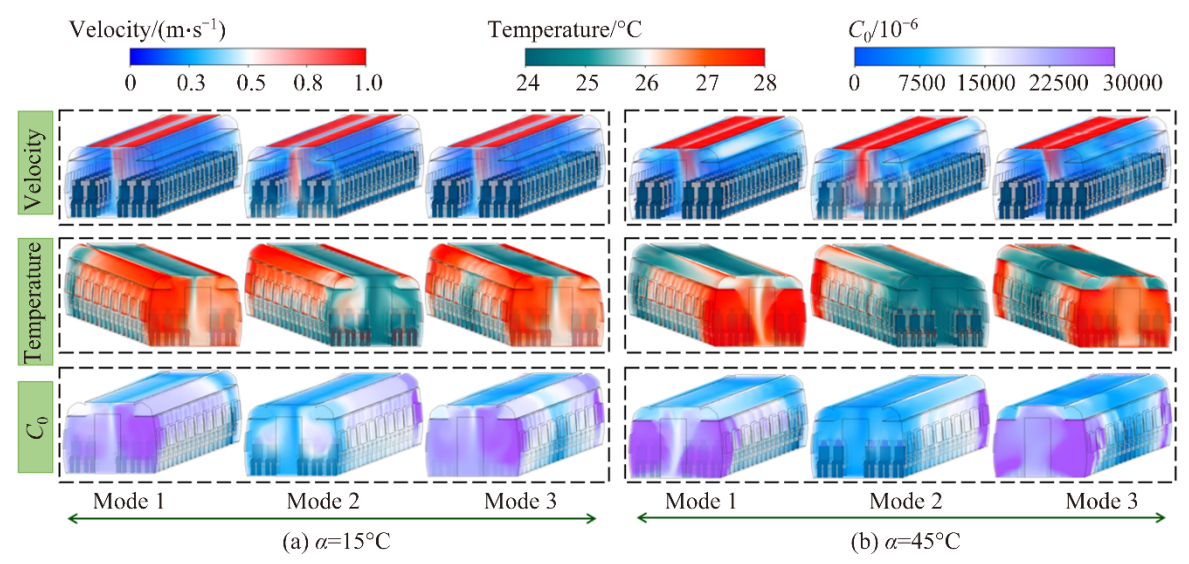


Figure S4 Distribution of velocity, temperature and pollutant concentration in the train cabin for different deflection modes: (a) α =15°; (b) α =45°

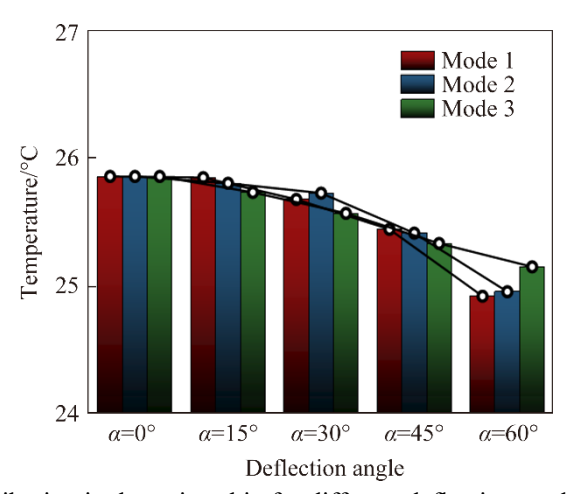


Figure S5 Mean temperature distribution in the train cabin for different deflection modes

Figure S6 illustrates the DR indices and non-uniformity coefficients in the train cabin for different deflection modes. As the deflection angle α increases, the regularity is the same for different deflection modes. The DR index, the velocity non-uniformity coefficient and the temperature non-uniformity coefficient in the passenger compartment all grow progressively with increasing α . The velocity non-uniformity coefficient fluctuates relatively more in mode 3. There is no significant difference in the non-uniformity coefficients for the remaining cases. Similarly, there is no significant difference in the DR indices for the 3 modes.

Figure S7 shows the pollutant concentrations and dispersion distances in the train cabin for different deflection modes. As the deflection angle α increases, the pollutant concentrations all show a gradual decrease, while the dispersion distances all show a gradual increase. In mode 1, the concentration of pollutants for passengers at the rear end of the cabin is relatively greater and spreads over a relatively longer distance. In mode 2, the regularity is the exact opposite of mode 1. In mode 3, the concentration of pollutants for passengers at the middle of the cabin is relatively greater and spreads over a relatively longer distance.

Two conclusions can be drawn from the analysis of the flow field characteristics and related evaluation indexes in the train cabin. First, both thermal comfort and air quality in the train cabin deteriorate with increasing deflection angle α for different deflection modes. Secondly, the flow field patterns and the regions of relative deterioration in the train cabin differ for different deflection modes.

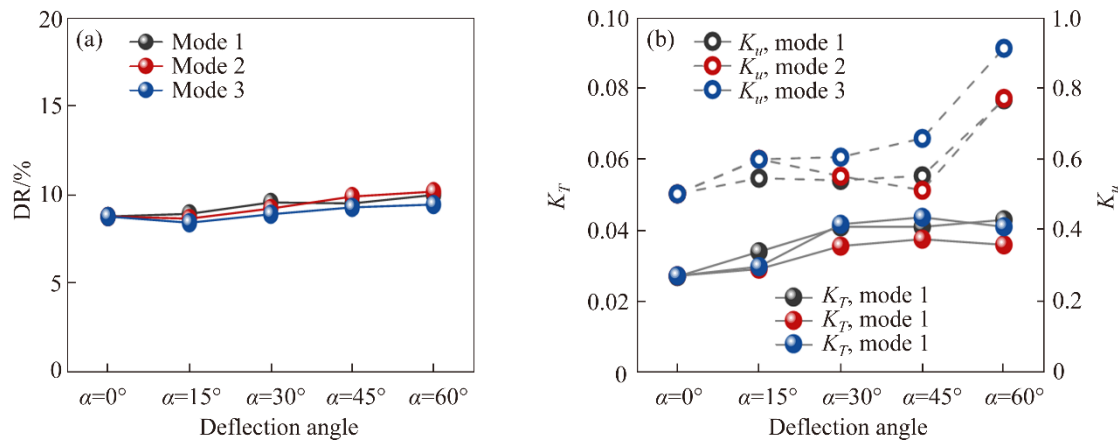


Figure S6 DR index and non-uniformity coefficients in the train cabin for different deflection modes: (a) DR index; (b) Velocity and temperature non-uniformity coefficients

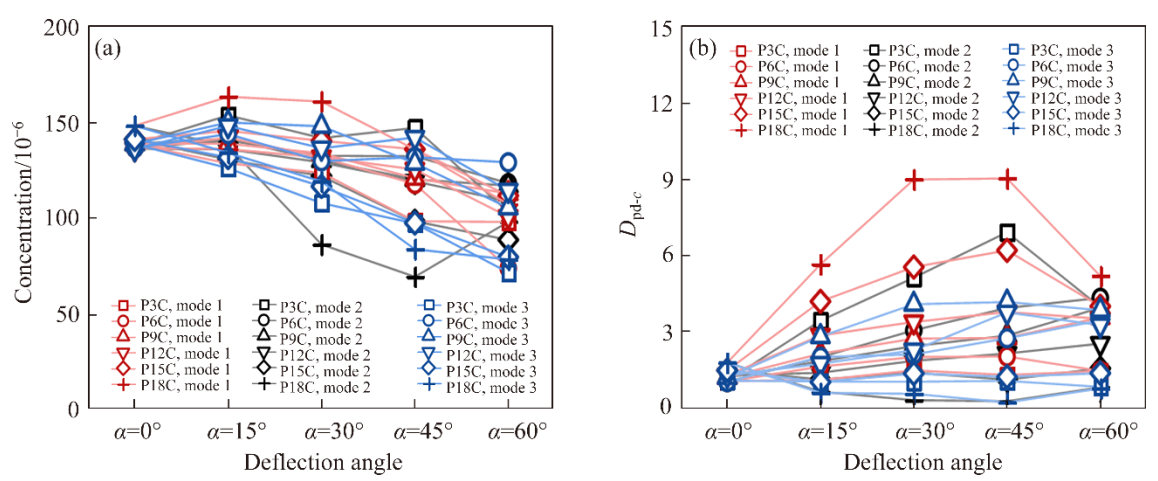


Figure S7 Pollutant concentrations and dispersion distances in train cabin under different deflection modes: (a) Pollutant concentrations; (b) Pollutant dispersion distances